TERRAIN-INDUCED SLUGGING

Mark McGuinness[1] and Robert McKibbin[2]

This paper has been reviewed and accepted for publication in the proceedings of the 2002 Mathematics-in-Industry Study Group held at the University of South Australia, Adelaide, Australia, 11-15 February 2002.

SANTOS Ltd is Australia's biggest supplier of natural gas. It operates nearly 600 wells, most of which are in South Australia. Generally the wells produce a mixture of raw, dense gas with some water and a kerosene-like condensate. These fluids pass through a compressor and are then pumped at high pressure through pipelines up to 180 km long to processing facilities. Both gas and liquid are carried in the one pipe, but they travel at different speeds.

At the outlet of the pipeline, the gas output is more or less steady, but the liquid flowrate varies considerably. This is due to the liquid travelling in the form of slugs, with the peak flows being up to 10 times the average; the slugs are often cyclic in nature. Slugging is a worldwide problem in pipelines carrying both liquid and gas. Not only does it make flows at the outlet difficult to handle, but it can induce severe mechanical vibrations in the pipe.

In pipes across undulating terrain, such as those operated by SANTOS, a major cause of slugging is the topography. Liquid tends to build up and sit at the lowest points of the pipeline, until it is forced onwards through the rest of the pipe by the pressure of the gas caught behind. See Fig. (1) for an illustration. SANTOS asked the MISG to develop a simple way of estimating peak liquid flow rates, slug sizes and the period between the peaks. The team concluded that the flow in downhill sections should be stratified with liquid and gas separated, whereas there would be a strong correlation between the length and slope of the uphill sections and the depth of the liquid in them.

[1]School of Math. & Comp. Sci., Victoria University of Wellington, PO Box 600, Wellington, NZ. Email Mark.McGuinness@vuw.ac.nz.

[2]Inst. Info. & Math. Sci., Massey Uni, Private Bag 102904, Albany, Auckland, NZ. Email R.McKibbin@massey.ac.nz.

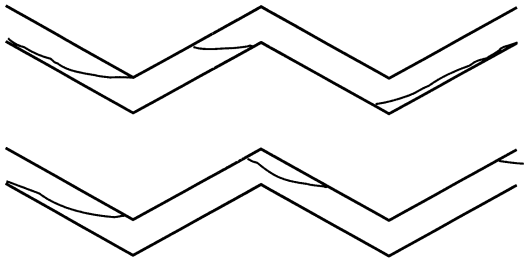

Figure 1: A sketch illustrating typical terrain-induced slugging, with the denser phase accumulating in elbows and uphill sections of pipe. Flow is from left to right.

1. Introduction

Slugging is a worldwide problem in pipelines carrying both liquid and gas, and is a particular problem in offshore wells. It makes control of flows at the outlet difficult, and may lead to shutting down of pipeline systems, at considerable expense.

Many mechanisms have been advanced for why slugging occurs, and different explanations may be valid for different pipelines. More than one mechanism may be acting at a time. But it is commonly assumed that in pipes across undulating terrain, such as those operated by SANTOS, a major cause of slugging is the topography itself. Liquid tends to build up and sit at the lowest points of the pipeline, until it is forced onwards through the rest of the pipe by the pressure of the gas caught behind.

Because of the expense and technical difficulty, there are no sensors in the SANTOS pipelines, and almost all the operational data comes from measurements taken at each end. So SANTOS asked the MISG to develop a simple way of estimating peak liquid flow rates, slug sizes and the period between the peaks. As an example with which to work, the company provided data on the 180-kilometre pipeline it operates between Ballera and Moomba in South Australia.

The team began with a general analysis of the problem. It found there was a more or less regular period of about 4 to 5 hours between peak liquid flows at the outlet, and that the form of the flow output resembled what would be expected

from two sine waves added together, suggesting the possibility of two dominant frequencies of slugging. Experimental and engineering experience suggested that slugging was due to the uphill segments of the pipeline, with the holdup (fraction of the flow area occupied by the lower layer) being larger on uphill sections. One possibility suggested was that the period between slugs was determined totally by the characteristics of the last uphill segment.

In addition to terrain, other mechanisms put forward to explain slugging included hydrodynamic reasons, where the different pressures and rates of flow of the gas and liquid induce waves in the liquid phase, some of which can be big enough to fill the pipe. This could be alleviated by increasing the diameter of the pipe or increasing the pressure or the pressure gradient under which the fluids flow.

The team was intrigued by the possibility that the equation for waves on shallow water developed by the Dutch mathematicians Korteweg and de Vries might be applicable, which would raise the possibility of the establishment of solitary waves and wave trains. The observed slugging period of 4.3 hours together with a fluid velocity of 0.4 m/s corresponds to a wavelength of about 6 km, while the depth of the liquid phase is a fraction of the pipe diameter of 0.4 m, so that the shallow-water approximation is a good one. However, it was eventually realised that there was no dispersive mechanism apparent, so that the KdV equation was not after all so relevant. Slugging might also be initiated by abrupt changes in the rate of output of the well or by starting up or shutting down the compressor and pump, thereby inducing transitions which moved along the pipeline either backwards or forwards.

One interesting fact uncovered by the team was that the time it would take the last uphill segment of the pipe before the outlet (about 800 m) to fill with liquid is about 3.4 hours, which is close to the cycle time of the slugging measured at the outlet (about 3 to 4 hours). So one possibility is that in addition to any slugging that might take place within the pipeline itself, the characteristics of the slugs at the outlet could be determined solely by the last uphill stretch.

The MISG team, however, concentrated on the impact of terrain. It noted that the pipe was of larger diameter than generally employed worldwide for such gas flows, and also that the gas itself was highly compressed, so that it was nearly as dense as the liquid phase. It appeared that the stratified flow could in this case be treated as liquid flowing over liquid rather than gas over liquid. The team began building a mathematical model of the pipeline system, exploring the operating conditions of the pipeline, and looking for simple approximate solutions. They started by looking at conditions and assumptions that would be necessary to build such a model.

Initially they decided on a model with two layers of incompressible liquid where the lower (denser) fluid flow is driven by the upper fluid due to the velocity contrast. The assumptions undelying this modelling are in Section 3. There would also be interactions, in the form of shear stresses, at the boundary between the fluids and the pipe, and between the fluids at their interface. The gas phase (the liquid on top) would flow much faster than the liquid below. The group then developed equations based on conservation principles (Section 3.1), and explored smooth (Section 3.1) and shock-wave (Sections 3.2 and 3.3) solutions for various regimes.

Owing to the complicated nature of the model equations and of the flows that can develop, the group was unable to find simple expressions for slug amplitude and period. However, a good foundation has been laid for further study of this model and of this challenging problem.

2. Two-phase pipeline flow

The pipeline from Ballera to Moomba is 180 km long and about 40 cm in diameter. It carries gas, condensate and water at high pressure (between 70 and 130 atmospheres) at about 1.5 kilometres per hour for the liquid and 15 kilometres per hour for the gas. There is no data on the actual conditions inside the pipe. What happens along the pipe has to be inferred on the basis of measurements collected at the end points and from the evidence of laboratory experiments conducted with glass channels. Flowrates measured at the output end, which show evidence of slugging in the liquid phase, are graphed in Fig. (2).

A set of simplified pipeline and flow data deduced from that provided by SANTOS is outlined in Table 1. For each flow layer, mean fluxes are used to calculate superficial velocities (based on the total pipeline cross-section) and these are used to calculate superficial Reynolds numbers. The latter indicate that the flows are in the high Re regime, and approximations may be made accordingly in the modelling and in the use of shear stress correlations.

3. A simplified model

After a good deal of discussion about the properties of the fluids flowing in the SANTOS pipelines, it was decided that the following assumptions could be made:

1. The flow generally consists of two layers of incompressible fluid, both liquid-like despite the lighter fraction usually being termed “gas”, with

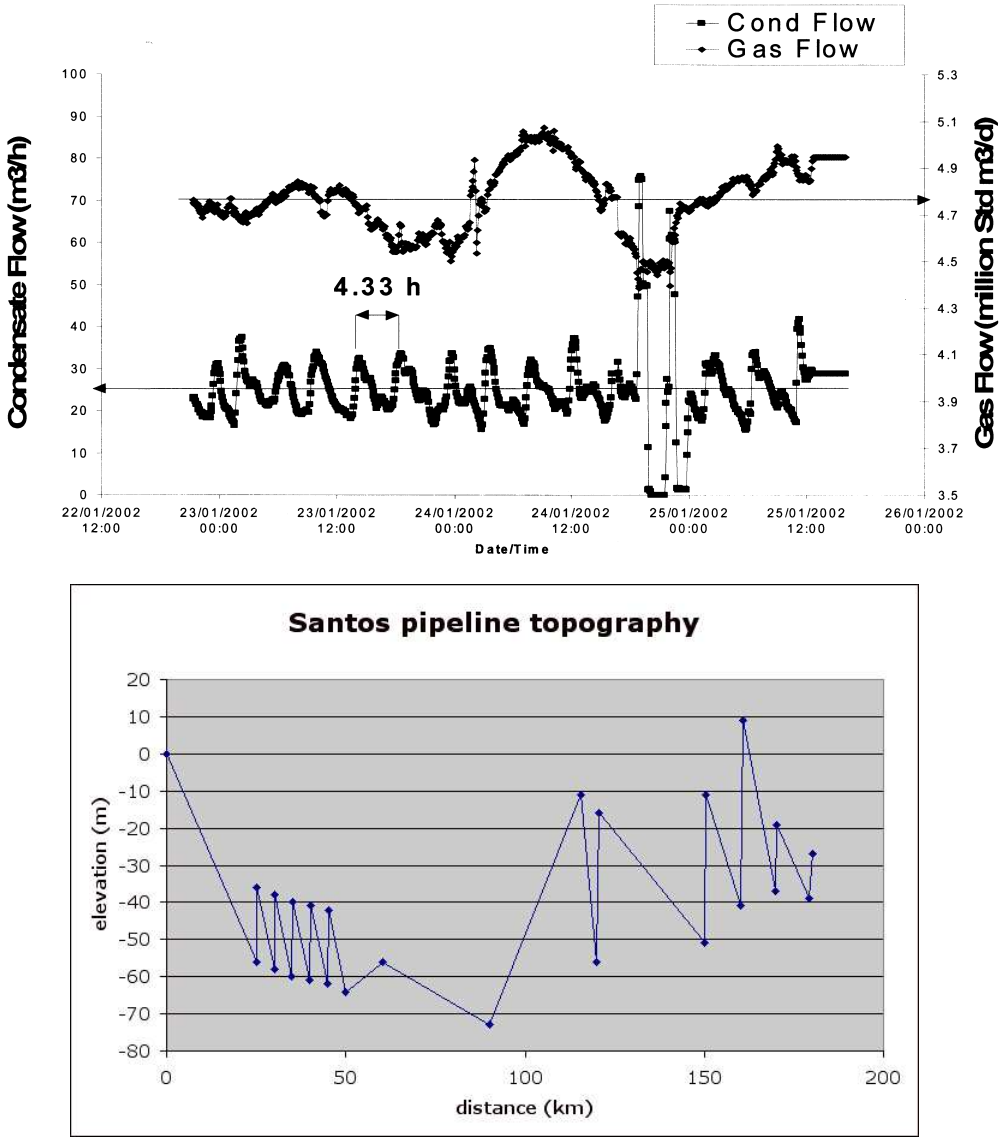

Figure 2: Graphs of flows at the pipeline outlet, and of the topography of the pipeline. The first graph is of the flowrates of gas and liquid phases measured at the separator at the outflow end of the pipeline from Ballera to Moomba, showing oscillating liquid flows (the lower data set) consistent with the presence of slug flow in the pipe. The upper data set shows that the gas phase does not exhibit comparable oscillations, in period or in magnitude. The second graph shows the topography of the pipeline - note the exaggerated vertical scale. The steepest sections of pipeline are at angles less than 6°. There has been no attempt to draw a smooth line between points, which are based on measurements of the elevation and distance along the pipe.

Table 1: Data from a typical pipeline installation, based on that from Ballera to Moomba, together with representative fluid properties.

Quantity	**Symbol**	**Value**	**Units**
internal pipe radius	R	0.200	m
internal pipe diameter	D	0.400	m
internal cross-sectional pipe area	$A_c = \pi R^2$	0.126	m^2
pipe length	L_p	180,000	m
pressure change along pipe	Δp	-5.5	MPa
average pressure gradient	$\overline{\frac{dp}{dx}} = \frac{\Delta p}{L_p}$	- 30	Pa m^{-1}
lower layer ("liquid")			
volume flux	Q_1	0.008	m^3 s^{-1}
density	ρ_1	550	kg m^{-3}
dynamic viscosity	μ_1	130×10^{-6}	kg m^{-1} s^{-1}
kinematic viscosity	ν_1	2.4×10^{-7}	m^2 s^{-1}
superficial velocity	$\overline{u_{1s}} = Q_1/A_c$	0.064	m s^{-1}
superficial Re	$\mathrm{Re}_{1s} = \overline{u_{1s}}D/\nu_1$	107,000	–
actual velocity	u_1	0.4	m s^{-1}
surface tension	γ	6.8×10^{-3}	N m^{-1}
upper layer ("gas")			
volume flux	Q_2	0.4	m^3 s^{-1}
density	ρ_2	140	kg m^3
dynamic viscosity	μ_2	18×10^{-6}	kg m^{-1} s^{-1}
kinematic viscosity	ν_2	1.3×10^{-7}	m^2 s^{-1}
superficial velocity	$\overline{u_{2s}} = Q_2/A_c$	3.17	m s^{-1}
superficial Re	$\mathrm{Re}_{2s} = \overline{u_{2s}}D/\nu_2$	10,000,000	–
actual velocity	u_2	4	m s^{-1}
drag function			
C Re^{-m}	C	0.046	–
	m	0.2	–

the more dense fluid flowing under the lighter layer. The Mach number is small, so internal gas shocks are not relevant phenomena and the densities of the fluid layers are, locally, uniformly constant. Fluid properties would change only slowly along the pipeline.

2. The pipeline slopes are small.

3. The interface between the layers is well-defined and generally has very small or zero gradient relative to the pipeline axis. The fluid velocity is closely parallel to the pipeline walls nearly everywhere, except perhaps at sudden transitions.

4. The calculated Reynolds number for each layer is high. (The "superficial Re" values shown in Table 1 are calculated using the superficial velocity values. The Re values based on actual mean velocities and hydraulic diameter will be typically of the same order as the superficial Re values.) Each layer flows with a nearly uniform velocity profile and with significant velocity variations (shear) only near the pipeline walls and the interface.

5. Cross-pipe pressure variations are close to hydrostatic, with axial pressure variation controlling the thermodynamic properties of the two phases. The axial pressure gradient is small, so phase changes on a local scale are ignored.

6. Transitions between flow regimes along the pipeline could be modelled as jumps which were stationary or travelled steadily either forwards or backwards along the pipe, with the interface heights and layer speeds in front being different from those behind.

7. The flows are driven by a net force resulting from a balance between pressure gradient and flow resistance caused by wall friction. The force on each layer is also affected by the shear between the layers at the interface.

3.1 Steady flow regions

The equations which describe the flow can be deduced from the standard mass, momentum and energy conservation equations. These are set out in various published works to which the group referred, and are not repeated here (see De Henau & Raithby, (1; 2; 3), Spedding (4), and Fozard (5)). In particular, Fozard sets out a system of equations which describe in detail the various simplifications and correlations which aid an attack on the problem. Some attention was paid by Fozard to current thinking on the quantification and characterisation of the shear stresses on the flow induced by the stationary pipeline surface, and by the interface between the layers.

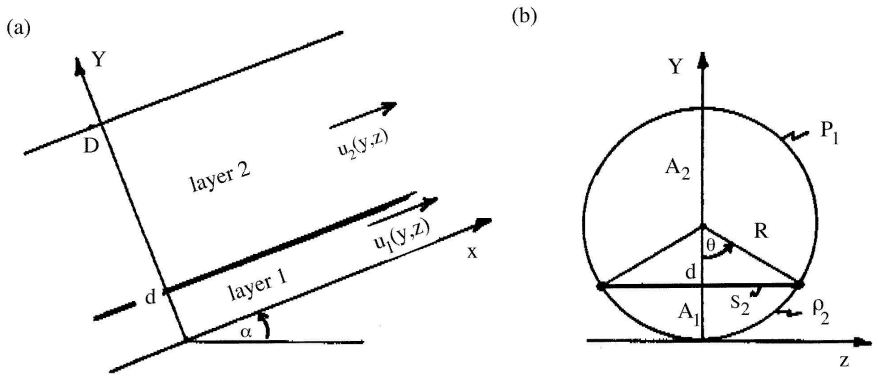

Figure 3: Lateral and cross-sectional views of the pipeline of diameter $D = 2R$. The interface is at height d above the bottom $(y, z) = (0, 0)$.

A simplified model where the flow is assumed to be locally steady and parallel to the pipe is considered here. Such sections of flow may be separated by stationary or moving "jumps" which feature abrupt changes in interface height. The pipeline slopes at an angle α to the horizontal in the direction of flow. In terms of a Cartesian (x, y, z) coordinate system with the x-axis along the bottom of the pipeline, y-axis in the vertical plane and z-axis horizontal (see Fig. (3)), the fluid velocity within each layer is of the form $\underline{v} = (u, v, w) = (u, 0, 0)$, where mass conservation and incompressibility ensures that $u = u(y, z)$. The corresponding Navier-Stokes (momentum conservation) equations are, in the x-, y- and z-directions respectively,

$$\frac{\partial p}{\partial x} = -\rho g \sin\alpha + \mu \nabla_2^2 u \ , \tag{1}$$

$$\frac{\partial p}{\partial y} = -\rho g \cos\alpha \ , \tag{2}$$

$$\frac{\partial p}{\partial z} = 0 \ , \tag{3}$$

where $\nabla_2 \equiv (0, \frac{\partial}{\partial y}, \frac{\partial}{\partial z})$. Using Equations (2) and (3), the pressures within the lower and upper layers are given by

$$p_1 = p_0(x) - \rho_1 g \cos\alpha \ y \quad \text{and} \quad p_2 = p_0(x) - \rho_1 g \cos\alpha \ d - \rho_2 g \cos\alpha \ (y - d) \ , \tag{4}$$

where $p_0 = p(x, 0, 0)$ is the pressure at the bottom of the pipe. The areal averages of the pressures within the flowing layers, each with respect to its flow cross-section, are

$$\overline{p_1} = \frac{1}{A_1} \iint_{A_1} p_1 dS = p_0(x) - \rho_1 g \cos\alpha \ R + \frac{2\rho_1 g \cos\alpha}{3A_1} [R^2 - (R-d)^2]^{3/2}$$

and

$$\begin{aligned}\overline{p_2} &= \frac{1}{A_2}\iint_{A_2} p_2 dS \\ &= p_0(x) - \rho_1 g\cos\alpha\ d - \rho_2 g\cos\alpha\ (R-d) - \frac{2\rho_2 g\cos\alpha}{3A_2}[R^2-(R-d)^2]^{3/2}\end{aligned}$$

and the total force exerted on the flow in the axial direction by the pressure is then $\overline{p_1}A_1 + \overline{p_2}A_2$. The corresponding areal integration of Equation (1) over a cross-section of the flow for layer 1 (note from Equation (4) that $\frac{\partial p_1}{\partial x} = \frac{d\overline{p_1}}{dx} = \frac{dp_0}{dx}$) leads to the following expression for the axial pressure gradient:

$$\frac{dp_0}{dx} = -\rho_1 g\sin\alpha + \frac{1}{A_1}\iint_{A_1} \mu_1 \nabla_2^2 u_1\ dS\ .$$

Using a variant of Green's theorem in the plane, this may be written as

$$\frac{dp_0}{dx} = -\rho_1 g\sin\alpha + \frac{1}{A_1}\int_{\partial A_1} \mu_1 \nabla_2 u_1 \cdot \underline{n}\ ds\ ,$$

where ∂A_1 is the boundary of the flow cross-sectional area A_1 in the $y-z$ plane. The line integral represents the net normal component of shear force at the edge of the lower flowing layer, part of which is in contact with the pipe wall, and part in contact with the upper flowing layer. This mean shear stress (tangential force per unit area) on the flow's surface may be divided into those two parts, and the equation written as

$$\frac{dp_0}{dx} = -\rho_1 g\sin\alpha + \frac{\tau_{1w}P_1 + \tau_{1I}S_I}{A_1}\ , \tag{5}$$

where τ_{1w} and τ_{1I} are the linearly-averaged mean shear stresses on the flow by the pipeline wall (perimeter P_1) and the interface between the fluid layers (width S_I) respectively. A similar process for the upper layer gives

$$\frac{dp_0}{dx} = -\rho_2 g\sin\alpha + \frac{\tau_{2w}P_2 + \tau_{2I}S_I}{A_2}\ . \tag{6}$$

The τ values may be expressed in terms of the fluid density, flow speed and Reynolds number for the flow in the form:

$$\tau = -\frac{1}{2}\rho U|U|C\ \mathrm{Re}^{-m}\ . \tag{7}$$

Here, U is the mean speed of the flow relative to that of the relevant boundary and C and m are (known) experimentally-determined parameters. The Reynolds number for each layer depends on the kinematic viscosity, the mean speed and

a typical length scale, usually the hydraulic diameter, for that layer. Fozard (5) explains that it is common practice to assume, when the upper layer is moving much faster than a lower, much denser layer, that the lower layer is an "open channel" flow and the upper layer a "closed pipe" flow. The hydraulic diameter used in the calculation of Re depends on the case assumed (see Table 2) while the mean speed of the flow for layer i is $\overline{u_i} = Q_i/A_i$.

Table 2: Parameters for flow geometry in terms of the pipeline radius R and the angle θ (the interface subtends an angle 2θ at the pipeline axis — see Fig. (3)).

Quantity	**Symbol**	**Formula**	**Units**
interface			
surface width	S_I	$2R\sin\theta$	m
lower layer			
depth	d	$R(1-\cos\theta)$	m
cross-sectional area	A_1	$(\theta - \sin\theta\ \cos\theta)R^2$	m^2
area fraction	$A = A_1/A_c$	$(\theta - \sin\theta\ \cos\theta)/\pi$	–
pipe contact perimeter	P_1	$2R\theta$	m
hydraulic diameter	D_{H1}	open : $4A_1/P_1$	m
		closed: $4A_1/(S_I + P_1)$	m
upper layer			
depth	$D - d$	$R(1+\cos\theta)$	m
cross-sectional area	A_2	$(\pi - \theta + \sin\theta\cos\theta)R^2$	m^2
area fraction	$1 - A = A_2/A_c$	$(\pi - \theta + \sin\theta\cos\theta)/\pi$	–
pipe contact perimeter	P_2	$2R(1-\theta)$	m
hydraulic diameter	D_{H2}	open : $4A_2/P_2$	m
		closed: $4A_2/(S_I + P_2)$	m

The shear stresses at the fluid layer interface must be equal and opposite, i.e. $\tau_{1I} = -\tau_{2I}$. Since the expression (7) for τ_{1I} and τ_{2I} will use different Re and ρ (density) values, even though the relative speed $U = \pm|u_1 - u_2|$ is the same in both expressions, the magnitudes of the calculated shear stress values will be different. Fozard explains that the appropriate value of interface shear to use is that calculated from the upper (faster) layer flow properties.

For a steady flow, the two axial pressure gradients given by Equations (5) and (6) must be equal. For given layer flow rates, the problem reduces to finding the interface level d (see Fig. (3) and Table 1) which provides equality. For given flow rates, small interface heights will lead to very large axial pressure gradient requirements for the lower layer, and relatively smaller values for the upper layer. This is reversed for interface positions near the top of the pipeline. Somewhere in between, there is an interface height d for which the axial pressure gradients required to maintain both flows against gravitational and shear forces are equal.

That value of d "solves" the problem.

A calculation using the parameter values given in Table 1 and for a zero pipeline slope ($\alpha = 0$) was made to find the value of the interface height which makes the axial pressure gradients for both layers the same. The calculated value of d is close to 0.044 m, and the corresponding axial pressure gradient is about -14 Pa m^{-1}. This compares with the overall average pressure gradient for the whole pipeline of -30 Pa m^{-1}; there must therefore be regions in the pipeline where the pressure gradient is significantly larger, so that the overall pressure drop matches the drop between inlet and outlet conditions. The calculated mean fluid speeds in lower and upper layers are approximately 1.1 and 3.4 m s^{-1} respectively, which are in the ranges of values provided by SANTOS during the workshop session. While these calculations were made after the MISG week, there is clearly some potential for further investigation along these lines, and such work is being continued by some members of the group.

3.2 Kelvin-Helmholtz instability

When two fluids move relative to each other as in this model, the interface is inherently unstable. This instability is generally called the Kelvin-Helmholtz instability (see, for example, Drazin and Reid (6)). The flow is unstable if (see Table 1 for symbols)

$$k\rho_1\rho_2(u_1 - u_2)^2 > g(\rho_1^2 - \rho_2^2) \ ,$$

where $g = 9.8$ m s^{-2} and k is the wavenumber (2π over the wavelength). We have ignored waves transverse to the pipe. Hence if $u_1 \neq u_2$ all short enough wavelengths are unstable. Using the parameter values in Table 1, the longest wavelength that is unstable is then $\sim$2m, too short to account for the Santos observations. If surface tension γ is added into the model, very short wavelengths are stabilised, and instability requires

$$\rho_1\rho_2(u_1 - u_2)^2 > 2(\rho_1 + \rho_2)\sqrt{g\gamma(\rho_1 - \rho_2)} \ .$$

We find that this condition is satisfied for our parameter values, and that the shortest unstable wavelength

$$\lambda = 2\pi\sqrt{\frac{\gamma}{g(\rho_1 - \rho_2)}}$$

is about 8mm, so that wavelengths between approximately 8mm and 2m are unstable according to the Kelvin-Helmholtz instability. Hence, while this does provide a mechanism for initiating jumps and transitions, it does not account for the observed slugging period.

3.3 Moving transitions

Another aspect considered was that where an abrupt change in flow conditions (a "jump") moves along the pipeline, separating two flow regimes each of which can be described by the analysis above. With the assumption that the transition moves at a constant speed V along a section where the pipeline slope remained constant, a frame of reference moving with the transition (see Fig.(4)) allows equations to be formulated which express conservation of mass and momentum flux through the "jump".

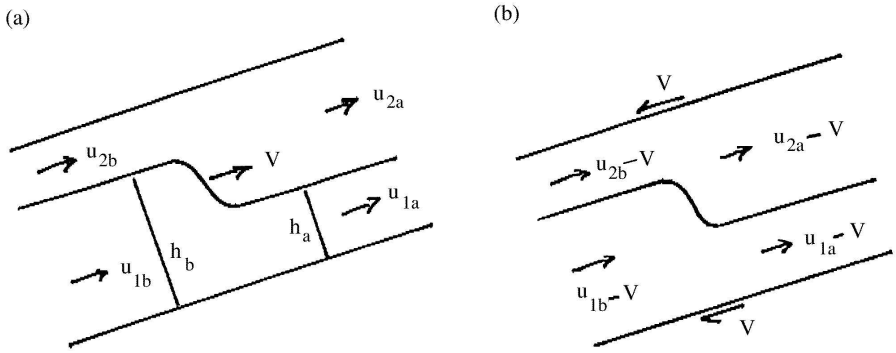

Figure 4: Schematic of a moving transition, speed V. (a) Speeds relative to a fixed frame of reference. (b) Speeds relative to the moving transition.

If the jump speed V is taken to be positive in the direction of the positive x-axis, the flow regime ahead of the jump is designated "ahead" (subscript a) and the regime behind is "behind" (subscript b). Conservation of mass (or volume, since the layers are incompressible) through the jump for the lower and upper layers gives, relative to the moving coordinate system,

$$\rho_1 A_{1b}(\overline{u_{1b}} - V) = \rho_1 A_{1a}(\overline{u_{1a}} - V) \ ,$$

and

$$\rho_2 A_{2b}(\overline{u_{2b}} - V) = \rho_2 A_{2a}(\overline{u_{2a}} - V) \ .$$

Attribution of the change in total axial momentum from "a" to "b" with the net pressure force across the jump (with the assumption that the jump region is short) gives:

$$\left[\rho_1(\overline{u_1} - V)^2 A_1 + \rho_2(\overline{u_2} - V)^2 A_2\right]_a - \left[\rho_1(\overline{u_1} - V)^2 A_1 + \rho_2(\overline{u_2} - V)^2 A_2\right]_b = [\overline{p_1} A_1 + \overline{p_2} A_2]_b - [\overline{p_1} A_1 + \overline{p_2} A_2]_a \ ,$$

or, that the modified momentum flux relative to the moving jump,

$$\left[\rho_1(\overline{u_1}-V)^2+\overline{p_1}\right]A_1+\left[\rho_2(\overline{u_2}-V)^2+\overline{p_2}\right]A_2\ ,$$

is conserved across the jump. For a given flow regime either ahead or behind such a transition, the above equations, together with the requirement that the axial pressure gradients for both layers within each region are equal (but will be different ahead and behind), are enough to uniquely solve for the jump speed V and the interface height in the other region. Such calculations may be useful in working out all possible flow states and transitions through the pipeline, without having to resort to massive CFD simulations.

3.4 Steady transitions

One other inferred possibility is that there can be stationary jumps at points in the pipeline, perhaps where there are slope changes due to topography. Such transitions would "link" different steady flow regimes, each of which would have to satisfy the condition that the axial pressure gradients within each layer were the same. Calculations comparing a horizontal pipeline section with sections which slope upwards or downwards with angle α, by solving equations (5) and (6) using the parameter values in Table (1), lead to the results in Table 3.

Table 3: Comparison of flows with the same fluxes but different pipeline slopes.

angle α (degrees)	axial pressure gradient (Pa m^{-1})	interface height d (m)	$\overline{u_1}$ (m s^{-1})	$\overline{u_2}$ (m s^{-1})
-1	+11.3	0.034	1.55	3.31
-0.5	-1.0	0.037	1.35	3.34
0	-13.8	0.044	1.05	3.39
+1	-69	0.16	0.17	5.1

It can be seen that very small pipeline slopes induce significant changes in axial pressure gradient. For negative slopes, the flow "runs away downhill" and is restrained by a positive pressure gradient, while a significant pressure drop is needed to maintain the "uphill" flow. In the latter case, the lower layer thickens (the "holdup" increases), and requires the faster-moving upper layer to "pull" it up the slope through increased interfacial shear. A downward slope of about 0.5° produces a flow where the gravitational and shear forces are nearly balanced, and the axial pressure gradient is close to zero.

Most of the values calculated above are within the ranges that were given by SANTOS from simulation data; the overall pressure gradient for the pipeline

is -30 Pa m^{-1}, while the lower and upper fluid speeds are in the ranges 0.2–0.5 m s^{-1} and 3–5.5 m s^{-1} respectively.

3.5 Choking

Complete choking of the flow was considered a possibility, especially since evidence from measurements made by SANTOS indicated large variations in liquid flow rates at the outlet. A simple calculation of the volume of the last section of the pipeline, which has a rise of 12m over its last 800m length, giving an upward slope of about 0.85°, showed that it would take a time of about 3.4 hours to fill it with the liquid phase at the indicated flowrate (see Table 1). The cycle time at the outlet was measured to be approximately 3 to 4 hours, so a choking effect may explain the phenomenon.

4. Conclusions and recommendations

The SANTOS problem is not an easy one. Oil and gas companies have devoted a large amount of resources to try to simulate the flow in pipelines, with a view to designing systems which have favourable characteristics only. The MISG group wrestled with the complications of current full mathematical models before deciding to try some very simple models which might reveal good descriptions of basic phenomena.

The angle of inclination of the pipeline is very important, with flow in downhill sections smoothing out to an evenly stratified behaviour, while flow in uphill sections develops slower and deeper condensate flows and has an increased probability of slugs forming. Given this, perhaps the most important section of a pipeline is the last section, and for smooth operating conditions this section should be slightly downhill, effectively operating as a separator and smoothing out any slugs that have developed in the previous downhill section. Such considerations, while of little help in controlling the existing setup, could affect decisions on future plant placement, for example.

The simple models described here were just part of the approaches considered by the MISG group. There was vigorous discussion about some subtle mathematical and modelling details, but these did not lead to immediately-obvious ways to proceed.

The problem remains. Some further investigations of points noted above may bear fruit.

Acknowledgements

The project moderators, Mark McGuinness and Robert McKibbin, would like to thank SANTOS Ltd representatives Tung Nguyen and Nigel Walker for the work they put into preparing the project and obtaining information for the participants. Their patience and willingness to answer what must have seemed the same questions over and over were impressive. The project working group (the "Sluggers") consisted of a small but persistent core and several others who contributed from time to time; it included Ellis Cumberbatch, Phil Howlett, Habib Alehossein, Tim Marchant, Stephen Lucas, William Cogill, Jim Hill, Grant Cox, Bernhard Neumann, John King, Peter Howell, Miriam Hochwald, Rebecca Weston and Chris Austin. All provided contributions to what was a most challenging but enjoyable attack on a difficult problem.

References

[1] De Henau, V., and Raithby, G.D., "A transient two-fluid model for the simulation of slug flow in pipelines — I. Theory", *Int. J. Multiphase Flow* **21** No.3 (1995) 335–349.

[2] De Henau, V., and Raithby, G.D., "A transient two-fluid model for the simulation of slug flow in pipelines — II. Validation", *Int. J. Multiphase Flow* **21** No.3 (1995) 351–363.

[3] De Henau, V., and Raithby, G.D., "A study of terrain-induced slugging in two-phase flow pipelines", *Int. J. Multiphase Flow* **21** No.3 (1995) 365–379.

[4] Spedding, P.L., and Spence, D.R., "Flow regimes in two-phase gas-liquid flow", *Int. J. Multiphase Flow* **19** No.2 (1993) 245–280.

[5] Fozard, J,. "Terrain slugging in near horizontal oilwells", Master of Science thesis, Jesus College, University of Oxford, September 2001.

[6] Drazin, P.G., and Reid, W.H., "Hydrodynamic Stability", Cambridge University Press, 1981.